

Article

Analytical Analysis of the Groundwater Drawdown Difference Induced by Foundation Pit Dewatering with a Suspended Waterproof Curtain

Kaifang Yang ^{1,2}, Changjie Xu ^{1,2,3,*}, Minliang Chi ^{1,2} and Pei Wang ⁴

¹ Research Center of Coastal and Urban Geotechnical Engineering, Zhejiang University, 866 Yuhangtang Road, Hangzhou 310058, China

² Center for Balance Architecture, Zhejiang University, 148 Tianmushan Road, Hangzhou 310012, China

³ State Key Laboratory of Performance Monitoring Protecting of Rail Transit Infrastructure, East China Jiaotong University, 808 Shuanggang East Road, Nanchang 330013, China

⁴ Department of Civil and Environmental Engineering, The Hong Kong Polytechnic University, 11 Hung Hom, Kowloon, Hong Kong 999077, China

* Correspondence: xucj@zju.edu.cn

Abstract: The dewatering of foundation pits with a suspended waterproof curtain causes different groundwater drawdowns inside and outside the pit, resulting in the drawdown difference between the inside and outside the pit. Maintaining a groundwater drawdown difference between the inside and outside of a foundation pit can eliminate the adverse effects of dewatering on the surrounding environment. According to previous studies on unsteady flow, an analytical solution of the groundwater drawdown with a suspended waterproof curtain under unsteady flow has been proposed. The analytical solution of unsteady flow and the formula of groundwater drawdown difference with a suspended waterproof curtain were validated by comparing pumping tests and finite-element method (FEM), in which a good agreement was observed. The magnitude of the drawdown difference generally represents the extent of surrounding groundwater affected by groundwater drawdown inside the pit. This paper also investigated the effects of sensitivity parameters on the drawdown difference for minimizing the effect of surrounding environment. During the process of dewatering with a suspended waterproof curtain, the groundwater drawdown (S_{it}) should not exceed the length of the waterproof curtain (L), and the optimal radius of foundation pit (R_w) and length of waterproof curtain (L) were found, i.e., $R_w/H_0 = 0.781$ and $L/H_0 = 0.813$ (H_0 is 32 m). Beyond these values, the drawdown difference tends to be stable. The drawdown difference is also significantly affected by the dewatering time. When $t < 48$ h, the groundwater drawdown difference decreases rapidly; when $t > 48$ h, the groundwater drawdown difference stabilizes.

Keywords: foundation pit dewatering; suspended waterproof curtain; phreatic aquifer; analytical method; drawdown difference



Citation: Yang, K.; Xu, C.; Chi, M.; Wang, P. Analytical Analysis of the Groundwater Drawdown Difference Induced by Foundation Pit Dewatering with a Suspended Waterproof Curtain. *Appl. Sci.* **2022**, *12*, 10301. <https://doi.org/10.3390/app122010301>

Academic Editor: Mingguang Li

Received: 20 September 2022

Accepted: 10 October 2022

Published: 13 October 2022

Publisher's Note: MDPI stays neutral with regard to jurisdictional claims in published maps and institutional affiliations.



Copyright: © 2022 by the authors. Licensee MDPI, Basel, Switzerland. This article is an open access article distributed under the terms and conditions of the Creative Commons Attribution (CC BY) license (<https://creativecommons.org/licenses/by/4.0/>).

1. Introduction

With the fast urbanization in many countries, a large number of underground infrastructures are constructed in central areas of cities [1–5]. During the construction of these underground infrastructures, foundation excavation is a complex process and requires special attention. Engineers should not only pay attention to the safety of adjacent buildings during excavation, but also need to appropriately pump out groundwater [6–9]. In recent years, as the excavation becomes deeper, the number of accidents related to foundation pit excavation is rising rapidly [10–12]. Particularly, it is reported that accidents caused by groundwater account for around 60% of total accidents [13–16].

Excavation usually adopts the dewatering scheme which pumps groundwater inside the foundation pit to work in dry conditions [17–20]. This process can improve the safety

of the foundation pit and increase stability of the soil around it, preventing flowing sand, piping effect and other related accident from happening. Foundation pit dewatering relies on the system of pumping wells and the waterproof curtain, and pumping wells can further be divided into two types: wells in the confined aquifer and wells in the phreatic aquifer [21,22]. In the past decades, most of research focus on wells in the confined aquifer, and mathematical models of a well in a confined aquifer were established based on the assumptions [23,24]. Wells in the confined aquifer lower the piezometric head of the confined aquifer to prevent water-inrush damage in the foundation pit [25–27]. On the other hand, wells in the phreatic aquifer need to consider more conditions when establishing mathematical models, which has always been a difficult problem [28,29]. Some scholars equate the mathematical model of a well in the confined aquifer to the model of a well in the phreatic aquifer [30,31]. However, the dewatering scheme is generally composed of several wells, forming a huge drawdown curve centered on the foundation pit, and the whole dewatering system is even more complex [32]. The dewatering scheme requires one to pump a large amount of groundwater to maintain the groundwater drawdown below the bottom of the pit with waterproof curtain [33]. At present, model tests about pumping groundwater are used to carry out the process of dewatering and investigate the mechanism of waterproof curtain, but these tests take more factors into consideration, which is likely to cause inaccurate results and this makes it difficult to acquire quantitative conclusions [34–36]. The finite-element method (FEM) has been used to simulate the dewatering process in foundation pits with waterproof curtains, which is convenient to directly simulate different dewatering conditions and to calculate groundwater drawdown [7,37,38]. However, this method cannot be directly applied for engineering design and construction. To save groundwater resources and protect adjacent buildings, it is essential to reasonably pump groundwater without affecting the surrounding environment [39–42]. Therefore, the prediction of the groundwater level around the pit during dewatering is an urgent problem to solve.

Particularly, in soils with thick phreatic aquifers, the groundwater is constantly recharged into the foundation pit, so the foundation pit needs to pump more than the expected amount of groundwater to maintain the groundwater level below the bottom of the pit. Most of the scholars focus on numerical analysis and model tests, but few of them investigate the mechanism of foundation pit dewatering from the analytical solution. In this study, an analytical solution to unsteady flow around a foundation pit located in a thick phreatic aquifer with the suspended waterproof curtain was derived by using Boltzmann transformation, and the formula of groundwater drawdown difference between the inside and outside of the pit was obtained. By investigating the sensitivity parameters on the groundwater drawdown difference, the conclusions of drawdown difference induced by dewatering inside the pit were used for providing a reference for the dewatering scheme in the thicker phreatic aquifer, which eliminates the adverse effects of dewatering on the surrounding environment.

2. Dewatering with a Waterproof Curtain

Dewatering is an important method to maintain the normal construction process in water-rich strata. Foundation pit dewatering often includes pumping wells and a waterproof curtain. The main function of the pumping wells is to maintain groundwater level below the bottom of foundation pit, while the waterproof curtain is to increase the seepage length and reduce or even prevent the inflow of groundwater into the foundation pit [43,44]. The waterproof curtain is divided into a closed waterproof curtain and suspended waterproof curtain. As shown in Figure 1a, the closed waterproof curtain is inserted into an impermeable layer to form a closed region. The application of the closed waterproof curtain can effectively improve the dewatering efficiency of the foundation pit and prevent the groundwater outside of the pit flowing into it. When the deep foundation pit is in a thicker phreatic aquifer, the closed waterproof curtain will increase the length of the waterproof curtain to cut off the hydraulic connection, which improves the reliability of construction.

In Figure 1b, the suspended waterproof curtain is not inserted into the impermeable layer. This type of curtain is used to weaken the influence of the seepage area by increasing the seepage path of groundwater and reach the goal of lowering the groundwater level. The main factors that affect the mechanism of the suspended waterproof curtain are the groundwater drawdown, the length of the waterproof curtain, the dewatering time, the permeability coefficient, etc. When the foundation pit is located in a thicker phreatic aquifer, a suspended waterproof curtain is more economical than closed waterproof curtain. In order to improve the dewatering efficiency, it is worthwhile to comprehensively investigate the effect of the suspended waterproof curtain on the groundwater drawdown. Therefore, this paper focuses on the variation of the drawdown difference induced by dewatering with the suspended waterproof curtain.

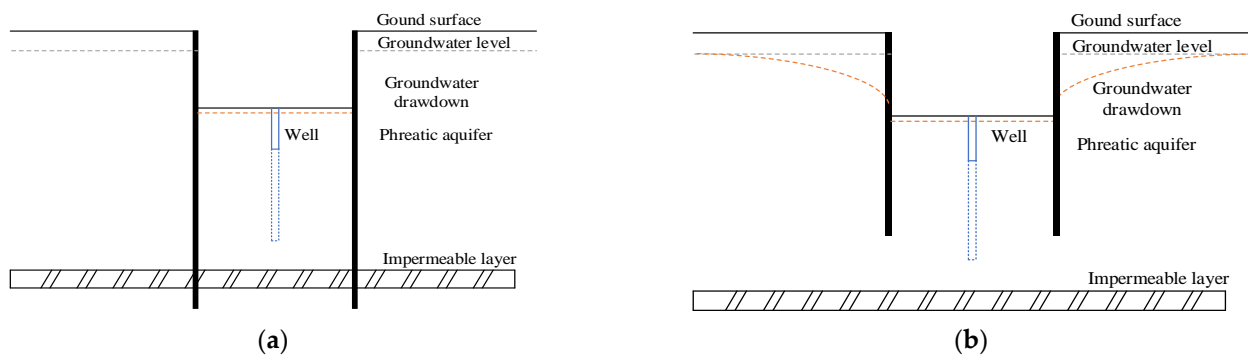


Figure 1. Schematic diagrams of foundation pit dewatering with waterproof curtain: (a) closed waterproof curtain, (b) suspended waterproof curtain.

3. Calculation of Groundwater Drawdown Difference

3.1. Methods and Assumptions

The dewatering process inside a foundation pit with a suspended waterproof curtain can be generally divided into two stages. In the first stage, the groundwater in the phreatic aquifer flows into the foundation pit through the opening between the end of the curtain and the impermeable layer. In the second stage, the groundwater flows upwards to the bottom of the pit as shown in Figure 2.

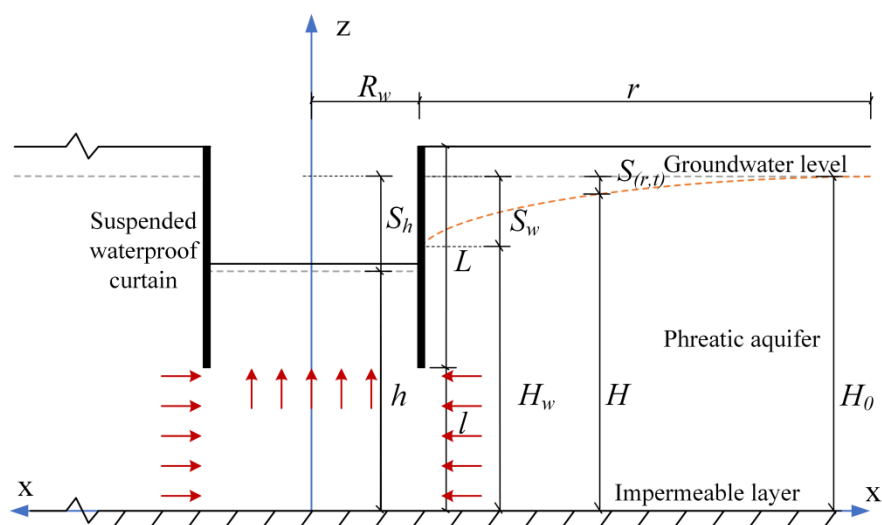


Figure 2. Diagram of foundation pit dewatering with a waterproof curtain and flow channels.

According to Groundwater Hydraulics [45,46], groundwater flows into the filtered screen of partially penetrating wells during the process of pumping. During the dewatering process, the deep foundation pit with a suspended waterproof curtain can be regarded

as a partially penetrating well with a large diameter. Therefore, the dewatering process of a foundation pit with the suspended waterproof curtain can be described with the formula of a partially penetrating well with a large diameter, corresponding to the first stage in dewatering.

In order to describe the dewatering process in a foundation pit with a suspended waterproof curtain, an analytical solution to the unsteady flow model is established [30,31], and the following assumptions are made: (1) The phreatic aquifer soil is homogeneous and isotropic, and extends indefinitely with uniform thickness. (2) Vertical flow is negligible. (3) The head within the well does not vary spatially. (4) The porous medium and fluid are slightly compressible. (5) The groundwater seepage follows Darcy's law. (6) The waterproof curtain and bottom of phreatic aquifer are impermeable. (7) Ignore the fluctuation of strata and the leakage from other aquifers. (8) The suspended waterproof curtain of the foundation pit can be regarded as a partially penetrating well with a large diameter.

3.2. Modeling a Partially Penetrating Well

According to the above assumptions, the unsteady flow governing equation for a large-diameter partially penetrating well can be obtained as

$$T \left(\frac{\partial^2 S}{\partial r^2} + \frac{1}{r} \frac{\partial S}{\partial r} \right) = S' \frac{\partial S}{\partial t} \quad (1)$$

where $a = T/S'$, T is the transmissivity; S' is the coefficient of storage.

The initial and boundary conditions are as follows

$$S(r, 0) = 0, \quad (0 < r < \infty) \quad (2)$$

$$S(\infty, t) = 0, \quad S(R_w, t) = S_w, \quad (t > 0) \quad (3)$$

$$\lim_{r \rightarrow R_w} \left(lr \frac{\partial S}{\partial r} \right) = \frac{Q_1}{2\pi K}, \quad (l > z > 0) \quad (4)$$

where R_w is foundation pit radius; r is the distance from the waterproof curtain; S_w is groundwater drawdown outside the waterproof curtain; S_h is groundwater drawdown inside the foundation pit; S is groundwater drawdown at any location outside the pit; t is pumping time; Q_1 is water inflow; K is the permeability coefficient. l is the distance between the bottom of the waterproof curtain and the impermeable layer.

The governing equation of groundwater to the unsteady flow can be transformed into time and space problems by using Boltzmann transformation [47,48]. The Boltzmann transformation reduces the equation for a contracting or expanding flow to the equation in spatially homogeneous system. This Boltzmann transformation method has also been applied in some studies on fully unconfined flow, and the partial differential equation can be transformed into ordinary differential equations, which simplify the groundwater flowing equation.

$$u = \frac{r^2}{4at} \quad (5)$$

Equation (6) can be obtained by substituting Equation (5) into Equation (1).

$$(1 + u) \frac{dS}{du} + u \frac{d^2 S}{du^2} = 0 \quad (6)$$

In order to calculate Equation (6), the boundary conditions of the ordinary differential equation can be obtained for a given time.

$$u_0 = \frac{r_w^2}{4at} \quad (7)$$

$$S|_{u \rightarrow \infty} = 0 \quad (8)$$

$$S|_{u \rightarrow u_0} = S_w \tag{9}$$

$$\frac{dS}{du} = e^{-C_1} \frac{e^{-u}}{u} = A \frac{e^{-u}}{u} \tag{10}$$

Equation (10) is calculated by integrals.

$$\int_{u_0}^{\infty} \frac{dS}{du} du = 0 - S_w = A \int_{u_0}^{\infty} \frac{e^{-u}}{u} du = AW(u_0) \tag{11}$$

$$A = -\frac{S_w}{W(u_0)} \tag{12}$$

$$\int_{u_0}^u \frac{dS}{du} du = S - S_w = A \int_{u_0}^u \frac{e^{-u}}{u} du = -\frac{S_w}{W(u_0)} \int_{u_0}^u \frac{e^{-u}}{u} du \tag{13}$$

$$W(u) = \int_u^{\infty} \frac{e^{-u}}{u} du, W(u_0) = \int_{u_0}^{\infty} \frac{e^{-u}}{u} du \tag{14}$$

where $W(u)$ is the well function.

At any time, the groundwater drawdown at different locations is shown in Equation (15).

$$S = S_w - \frac{S_w}{W(u_0)} \int_{u_0}^u \frac{e^{-u}}{u} du = S_w \frac{W(u)}{W(u_0)} \tag{15}$$

Based on Darcy’s law and Dupuit’s assumption, the slope of the groundwater drawdown for a well is regarded as the hydraulic gradient. The multiplication of the slope and the soil permeability coefficient is considered to be the flow rate. The multiplication of the flow rate and the area of water passing a section of a partially penetrating well is the water inflow. Therefore, the groundwater inflow Q_1 of a partially penetrating well with a large diameter can be obtained from Equation (16).

$$Q_1 = 2K\pi rl \frac{\partial S}{\partial r} |_{r \rightarrow R_w} = 4K\pi l \frac{S_w e^{-u_0}}{W(u_0)} \tag{16}$$

3.3. Modeling the Flow of Groundwater into the Foundation Pit

The seepage path satisfies the above assumptions, and water head at any location within the foundation pit needs to satisfy the assumption of constant head. The length of seepage path of groundwater flowing into the bottom of the foundation pit is calculated as

$$(h - l) + (H_w - l) = h + H_w - 2l \tag{17}$$

where h is the groundwater level in the foundation pit, H_w is the groundwater level outside the foundation pit, and l is the distance between the bottom of the waterproof curtain and the aquitard layer.

The rate of groundwater flowing into the foundation pit can be re-written as

$$Q_2 = k\pi R_w^2 \frac{H_w - h}{H_w + h - 2l} \tag{18}$$

3.4. The Connection of the Groundwater Drawdown between Inside and Outside the Foundation pit

It is known that the flow rate of groundwater outside the pit is equal to that inside the pit. In other words, Q_1 from Equation (16) and Q_2 from Equation (18) should have the same value.

Therefore, the groundwater level in the foundation pit can be expressed as

$$h = \frac{H_w R_w^2 W(u_0) - 4l e^{-u_0} (H_w - 2l) (H_0 - H_w)}{R_w^2 W(u_0) + 4l e^{-u_0} (H_0 - H_w)} \tag{19}$$

Then, the drawdown difference Δ with a suspended waterproof curtain is

$$\Delta = H_W - h \quad (20)$$

where H_0 is the thickness of phreatic aquifer.

In this section, Boltzmann transformation is introduced to solve the problem on an analytical solution to unsteady flow, and the calculation formula of the groundwater inflow is obtained. According to law of conservation of mass, a formula for calculating the difference between the groundwater level inside and outside the foundation pit is proposed. This formula is related to time, length of the waterproof curtain, groundwater drawdown, and other parameters, e.g., $\Delta = 0$ when $t = 0$ h, the application of Equation (19) calculates that $h = H_w$. The foundation pit has not started to pump groundwater, and this results in the groundwater being at the same water level, which is consistent with the condition of foundation pit dewatering.

4. Model Validation

4.1. Project Information

The case used in this study is the station of Nanchang Metro Line NO.4 in Jiangxi Province as shown in Figure 3. The open excavation method is used for the station. The surrounding environment of the excavation is relatively complex; there are some buried pipelines and adjacent buildings with a pile foundation around the station. This foundation pit is 238 m in length and 22.7 m in width, and the excavation depth is 16.0 m. The underground diaphragm wall and internal support system were adopted for this station. The underground diaphragm wall is a reinforced concrete structure with a thickness of 800 mm. The internal support system consists of one reinforced concrete support and two steel supports as shown in Figure 4. The elasticity modulus of the underground diaphragm wall, the reinforced concrete support, and the steel support are 35 GPa, 30 GPa, and 200 GPa, respectively.



Figure 3. Nanchang Metro Line NO.4.

Nanchang has a subtropical monsoon climate with abundant rainfall and widespread lakes and groundwater. The foundation pit is mainly affected by the phreatic aquifer, which is located in silty clay ③-1, fine sand ③-2 and coarse sand ③-4. Because sandy soil has the large gravitational water release characteristic, excavation may cause landslides, sand flow and other adverse phenomena if no measures are taken to decrease the moisture content of the soil layer. Soil properties of the different layers are shown in Table 1.

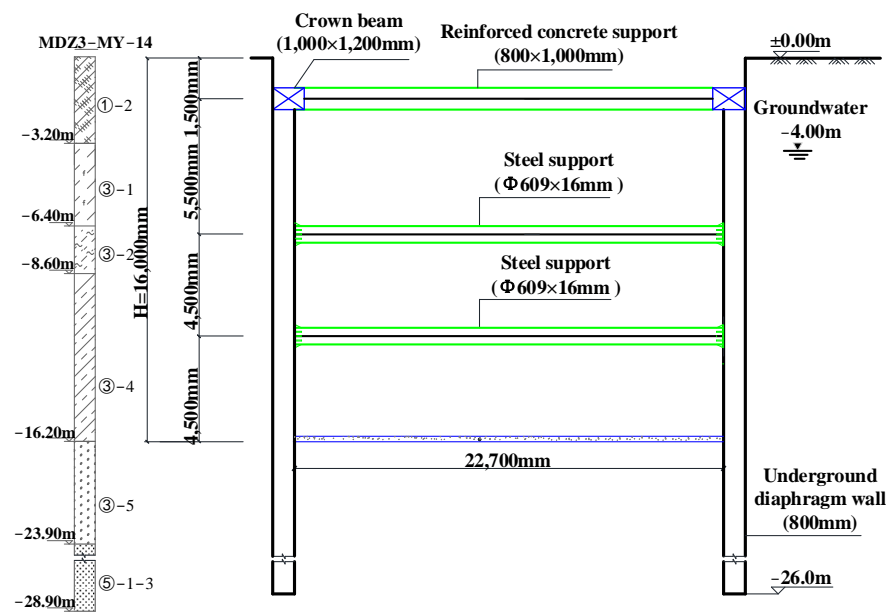


Figure 4. Section of foundation pit with retaining structure.

Table 1. Physical and mechanical parameters of soils.

Soil Stratum	Soil Number	Unit Weight γ (kN/m ³)	Cohesion c (kPa)	Internal Friction Angle φ (°)	Modulus of Deformation E_0 (MPa)	Permeability Coefficient K (m/d)
Fill	①	18.5	12	10	5.7	5
Silt clay	②-2	18.0	6	2	7	0.003
Silty clay	③-1	18.8	33	12	18	0.004
Fine sand	③-2	19.6	2	28	23	15
Medium sand	③-3	19.7	1	31	29	40
Coarse sand	③-4	19.8	1	34	32	80
Gravelly sand	③-5	20.0	1	36	33	100
Rounded gravel	③-6	20.5	1	38	35	120
Weathered rock	⑤-1-3	23.9	350	32	70	0.1

4.2. Pumping Test

One pumping well and two observation wells were used to conduct the single-well pumping test of the partially penetrating well in the phreatic aquifer. The test parameters are shown in Table 2. The test was divided into three stages, and the groundwater drawdowns are 1.21 m, 2.65 m, and 3.93 m, respectively. The results of the pumping test are shown in Table 3 and Figure 5. The groundwater drawdown in the observation wells decreased with the groundwater drawdown in the pumping well. The maximum groundwater drawdown was close to the pumping well, while the minimum value was far away from the pumping well. With the increase of time, the groundwater level first dropped sharply and then stabilized. The permeability coefficient in the phreatic aquifer is calculated based on the test results using the following equation (the Industrial Standard DL/T 5213-2005 of China, 2005) [49].

$$K = \frac{0.732Q}{(2H - s_1 - s_2)(s_1 - s_2)} 1g \frac{r_2}{r_1} \quad (21)$$

where r_1 and r_2 are the distances between the pumping well and the observation wells, respectively; s_1 and s_2 are the groundwater drawdown of the observation wells.

Table 2. Parameters of pumping test.

Name	Value
Groundwater type	Phreatic aquifer
Radius of pumping well	0.1 m
Length of pumping well	9.5 m
Pumping time	8 h
r_1	5 m
r_2	10 m

Table 3. Results of pumping test.

Test Stratum	Groundwater Drawdown S_w (m)	Water Inflow Q (m ³ /d)	Calculated Value K (m/d)
Coarse sand ③-4	1.21	176.8	52.4
Gravelly sand ③-5	2.65	360.3	62.1
③-5	3.93	471.4	57.8

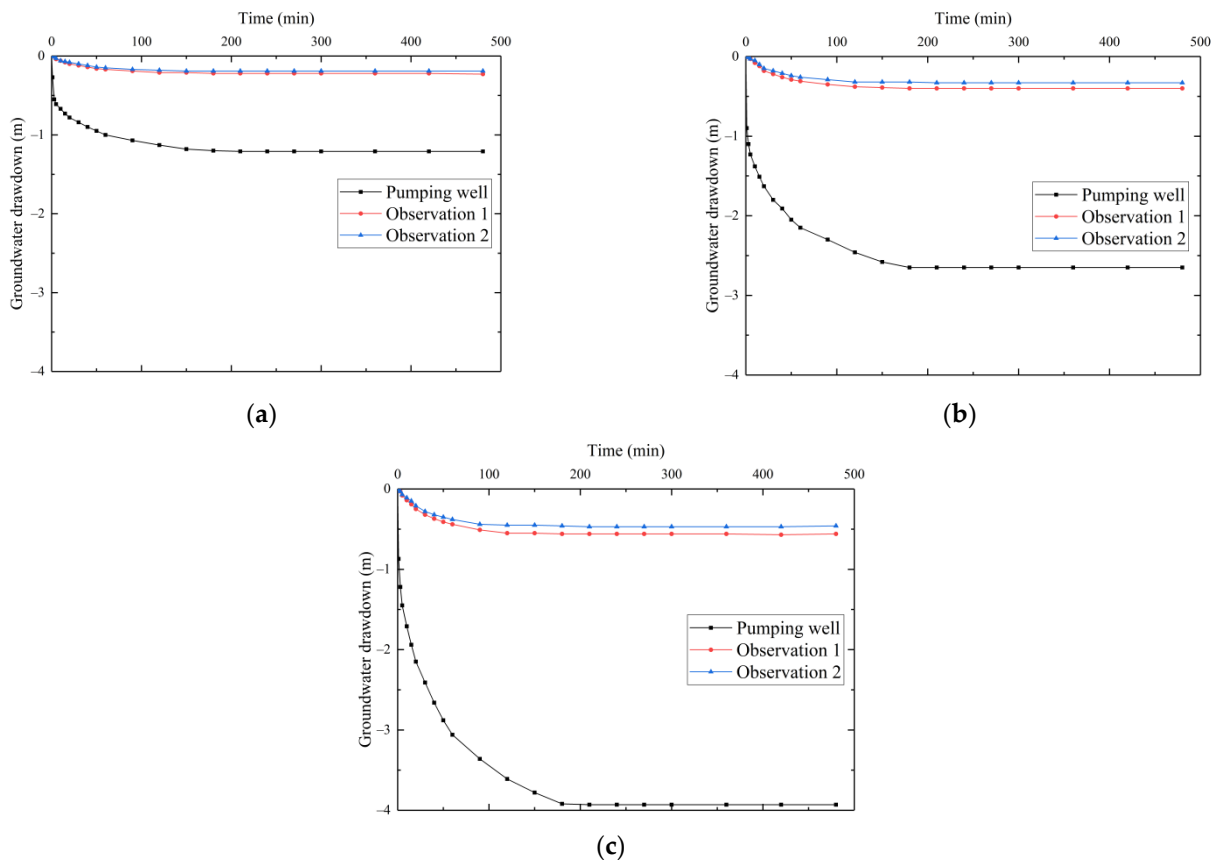


Figure 5. Results of pumping tests: evolution of groundwater drawdown in the pumping well and the observation wells; (a) first groundwater drawdown is 1.21 m, (b) second groundwater drawdown is 2.65 m, (c) third groundwater drawdown is 3.93 m.

4.3. FEM Model Setup

Based on the finite-element method (FEM), the numerical models of the single-well pumping test (model A in Figure 6) and dewatering with a suspended waterproof curtain (model B in Figure 7) were established. Both models have a dimension of 400 m in diameter and 30 m in thickness, and the thickness of the aquifer is 26 m. The initial groundwater level is 4 m below the ground surface, the radius of the pumping well is 0.1 m, the filter length of pumping well is 9.5 m, pumping time is 4 h, and the permeability coefficient is

57.8 m/d during the pumping test. The applied constitutive model of soil is the Hardening Soil model with small-strain stiffness; the parameters of the constitutive model are shown in Table 4. The radius of foundation pit is 10 m during dewatering with the suspended waterproof curtain, and other parameters are shown as above. Key features of the two models are summarized as follows:

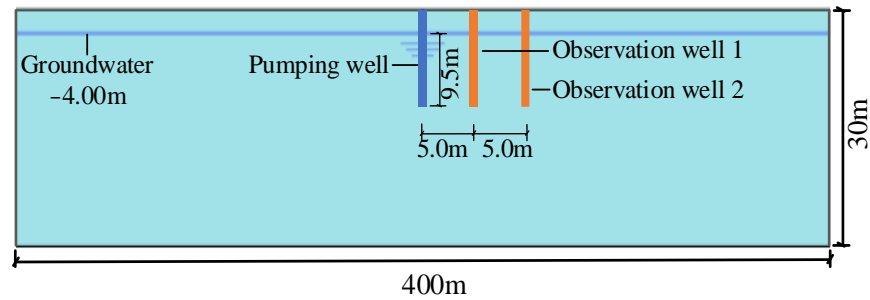


Figure 6. Numerical model A: single pumping well.

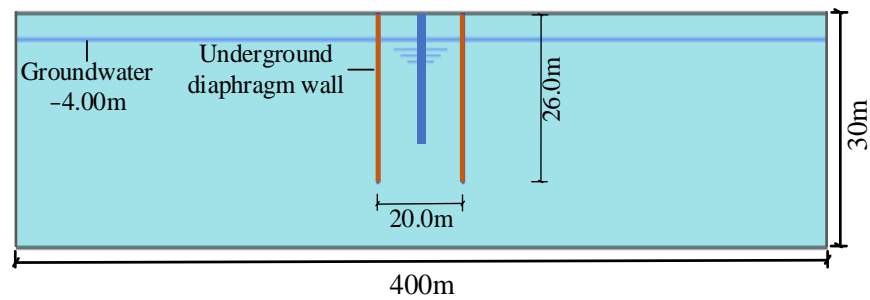


Figure 7. Numerical model B: dewatering in the foundation pit with suspended waterproof curtain.

Table 4. The parameter of the constitutive model.

γ_{unsat} (kN/m ³)	c' (kPa)	ϕ' (°)	Ψ (°)	E_{50}^{ref} (kN/m ²)	E_{oed}^{ref} (kN/m ²)
18.0	7	30.7	0	25,000	25,000
E_{ur}^{ref} (kN/m ²)	m	ν	P_{ref} (kPa)	R_f	G_0^{ref} (kN/m ²)
75,000	0.7	0.2	100	0.9	150,000

Model A. The numerical model was established to simulate the single-well pumping test. The model A activates the well structure to simulate the process of pumping at groundwater drawdowns of 1.21 m, 2.65 m, and 3.93 m.

Model B. The groundwater drawdown needs to be lowered by 12 m when the foundation pit is excavated. Therefore, the groundwater drawdown of model B lowers to −16 m. The groundwater seepage process was simulated by activating the well structure, plate structure and interface element.

4.3.1. Validation of Groundwater Drawdown

Groundwater drawdown at different locations during a pumping test from Equation (15), the field measured data, and the FEM simulation (Model A) are compared in Figure 8. It can be seen from Figure 8 that the groundwater drawdowns predicted by different methods during the pumping test are in good agreement, and the influence areas of the pumping test are also consistent. During the pumping test, the soil layer near the pumping well is not homogeneous and may have different hydraulic or mechanical properties. The analytical solution and the numerical model, however, assume the soil layer to be homogeneous, which leads to larger groundwater drawdown than the measured data

(Vilarrasa et al., 2011; Anwar, 2018). When the groundwater drawdown increases, the difference among the measured values, the calculated values and the simulated values of pumping test gradually narrows.

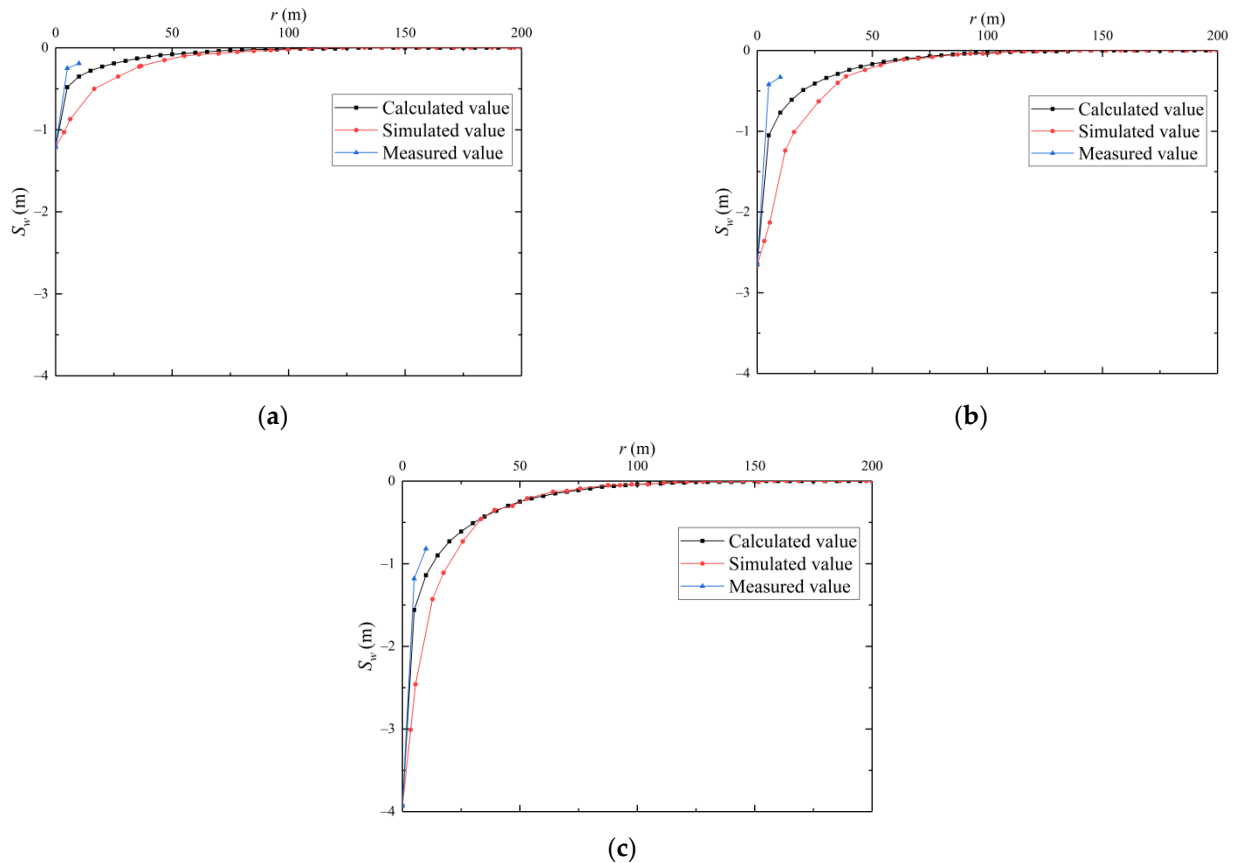


Figure 8. The groundwater drawdown at different locations when S_w equals to 1.21 m (a), 2.65 m (b), and 3.93 m (c).

When the pumping well is pumping groundwater, the nearby groundwater level is seriously affected by the pumping well and rapidly decreases, and the drawdown curve gradually stabilizes with the increase of distance. The influence areas of the pumping test increase with the groundwater drawdown; the influence areas increase from 70 m to 100 m when the groundwater drawdown increases from 1.21 m to 3.93 m.

4.3.2. Validation of Groundwater Drawdown Difference

With a groundwater drawdown of 12 m inside the pit, the groundwater drawdown difference obtained from the analytical method and Model B are compared in Figure 9. As shown in Figure 9, the distribution of groundwater drawdown outside the pit according to Equations (15) and (19) are consistent with the simulated results with similar influence areas.

The groundwater drawdowns outside the waterproof curtain from the analytical method and the FEM simulation are -3.40 m and -3.78 m, respectively, corresponding to drawdown differences of 8.60 m and 8.22 m. Such a small difference in the drawdown difference between the analytical method and the simulation, i.e., 11.76%, verifies the validity of the analytical method.

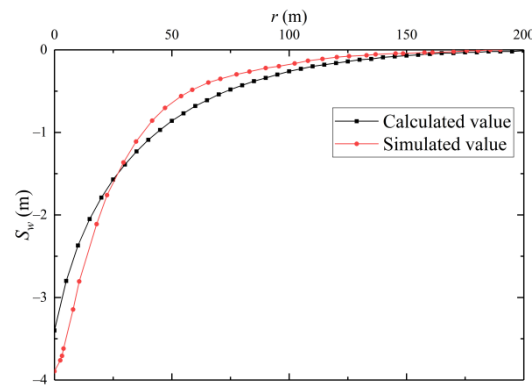


Figure 9. Groundwater drawdown outside the pit at different locations with S_w equal to 12 m.

5. Discussion on Sensitivity Parameters

The magnitude of the drawdown difference generally represents the extent of surrounding groundwater affected by groundwater drawdown inside the pit. A large drawdown difference means that the groundwater level outside the pit is lowered much slower than that inside the pit during dewatering, which imposes a very slight effect on the surrounding environment. On the other hand, when both the groundwater level inside and outside the pit decreases quickly, the magnitude of groundwater drawdown difference is small, indicating significant water flow from the surrounding soils into the pit. To investigate the effects of the groundwater drawdown inside the pit (S_h), the radius of the foundation pit (R_w), and the length of the waterproof curtain (L) on the groundwater drawdown difference, a series of sensitivity analyses were conducted using the proposed analytical method. Note that these sensitivity parameters were made dimensionless for simplicity, as shown in Table 5.

Table 5. Combination of the sensitivity parameters ($H_0 = 32$ m).

Names	S_h/H_0	R_w/H_0	L/H_0
Effect of S_h	(0.063–0.563)	0.313	0.844
			0.688
			0.531
Effect of R_w	0.375	(0.063–1.250)	0.844
			0.688
			0.531
Effect of L	0.375	0.313	(0.438–0.938)
		0.625	
		0.938	

5.1. Effect of S_h

The effect of S_h on the drawdown difference is presented in Figure 10. When the groundwater drawdown inside the pit ranges from 2 m to 18 m with an increment of 2 m S_h/H_0 ranges from 0.063 to 0.563. Since the groundwater outside the waterproof curtain cannot be recharged to the foundation pit in time, the groundwater level outside the waterproof curtain will be at a high level, and the drawdown difference will gradually increase.

When L/H_0 decreases from 0.844 (Figure 10a) to 0.688 (Figure 10b), the seepage path of groundwater is also decreased. As a result, groundwater outside the waterproof curtain can quickly flow into the pit, and the drawdown difference gradually decreases. Figure 10a shows that as S_h/H_0 increases from 0.063 to 0.563, $L/H_0 = 0.844$ causes the largest range of groundwater difference, and Δ/H_0 increases from 0.043 to 0.268 when $t = 192$ h, Δ/H_0 increases by 0.225.

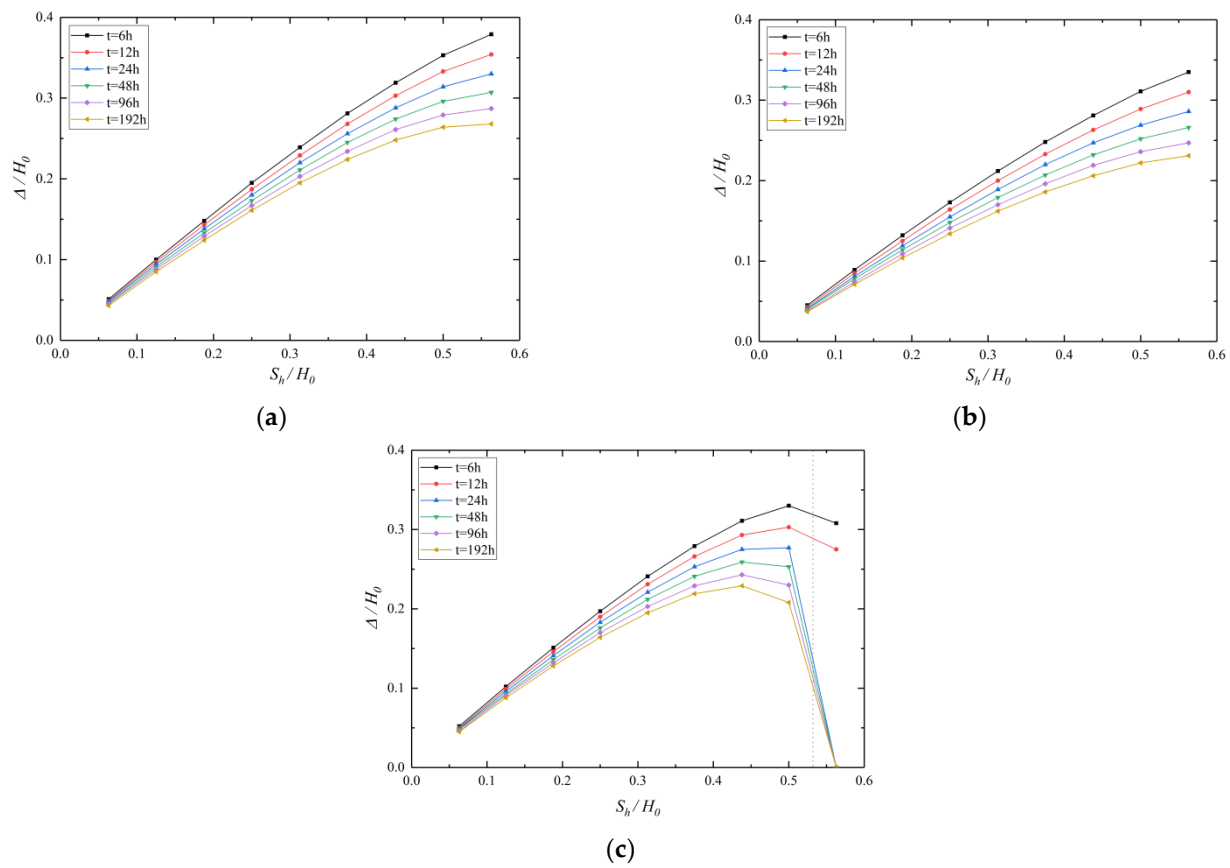


Figure 10. Effect of S_h on the groundwater drawdown difference: (a) $L/H_0 = 0.844$, (b) $L/H_0 = 0.688$, (c) $L/H_0 = 0.531$.

As shown in Figure 10c, when the S_h/H_0 exceeds L/H_0 , the groundwater difference decreases, which can be explained by a change of dewatering patterns and water level distribution according to Xu et al. (2014). When $S_h/H_0 > L/H_0$, the effect of the waterproof curtain extending the seepage path becomes weaker, and it is not appropriate to adopt the scheme of groundwater drawdown being greater than the length of the waterproof curtain.

5.2. Effect of R_w

To focus on the effect of R_w , the groundwater drawdown S_h/H_0 and the thickness of the aquifer H_0 were set to 0.375 and 32 m, while other parameters were unchanged as described above. As shown in Figure 10, the variation curve of drawdown difference is obtained by the calculation formula with the radius of the pit. As the radius of the pit increases from 2 m to 40 m, corresponding to an increase of R_w/H_0 from 0.063 to 1.250, the drawdown difference shows a decreasing trend. When R_w/H_0 is in the range from 0.063 to 0.781, the drawdown difference decreases quickly with the increase of R_w/H_0 . When R_w/H_0 is larger than 0.781, the effect of radius of the foundation pit on the groundwater drawdown outside the pit is very slight.

When L/H_0 decreases from 0.844 (Figure 11a) to 0.531 (Figure 11c), the drawdown difference gradually decreases. Figure 11a shows that as R_w/H_0 increases from 0.063 to 1.250, $L/H_0 = 0.531$ causes the largest range of drawdown difference, and as Δ/H_0 decreases from 0.357 to 0.029 when $t = 192$ h, the Δ/H_0 decreases by 0.328. If the larger drawdown difference is maintained, it is recommended to adopt the scheme of small radius of the foundation pit.

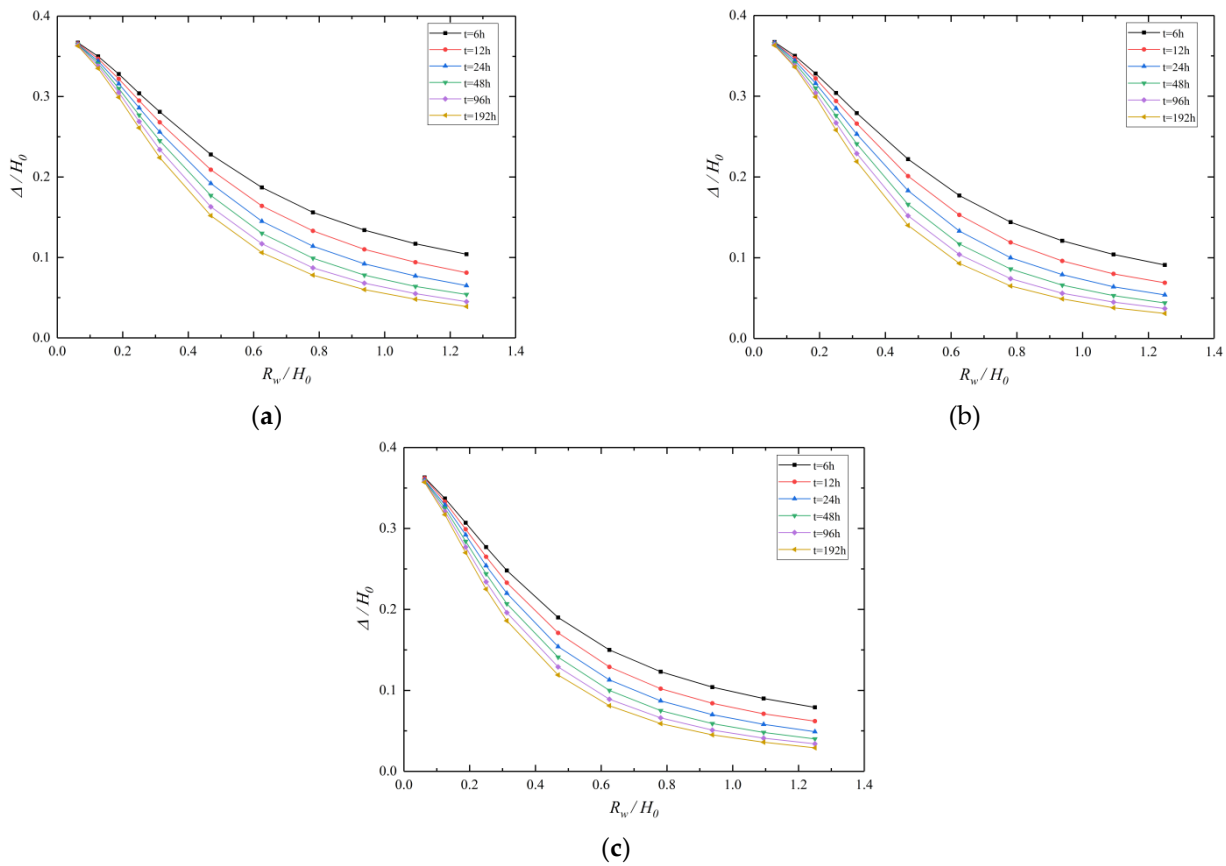


Figure 11. Effect of R_w on the groundwater drawdown difference: (a) $L/H_0 = 0.844$, (b) $L/H_0 = 0.688$, (c) $L/H_0 = 0.531$.

5.3. Effect of L

As the length of waterproof curtain increases from 14 m to 30 m, corresponding to L/H_0 ranging from 0.438 to 0.938, the drawdown difference first increases and then stabilizes, which can be explained by the increase of the groundwater seepage path. When $L/H_0 > 0.813$, the drawdown difference tends to be stable, indicating the optimal length of waterproof curtain to effectively maintain the drawdown difference.

When R_w/H_0 increases from 0.313 (Figure 12a) to 0.938 (Figure 12c), the drawdown difference decreases rapidly. Figure 12a shows that as L/H_0 increases from 0.438 to 0.938, $R_w/H_0 = 0.313$ causes the largest range of difference, and as Δ/H_0 increases from 0.113 to 0.227 when $t = 192$ h, Δ/H_0 increases by 0.114. If the larger drawdown difference is maintained, it is recommended to adopt the scheme of a larger length of waterproof curtain.

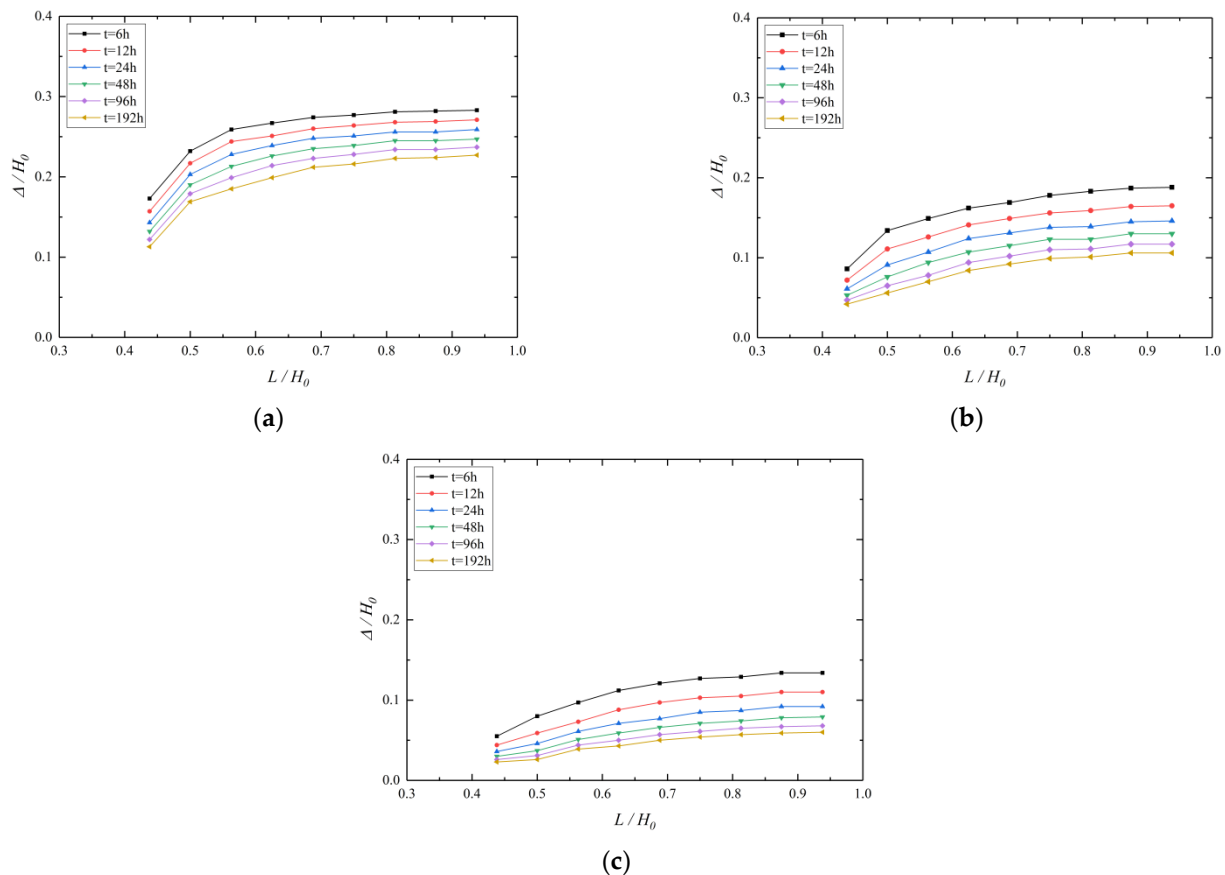


Figure 12. Effect of L on the groundwater drawdown difference: (a) $R_w/H_0 = 0.313$, (b) $R_w/H_0 = 0.625$, (c) $R_w/H_0 = 0.938$.

5.4. Effect of t

The analytical method obtained from this paper was used to calculate the groundwater drawdown difference induced by dewatering time under the unsteady flow, and the dewatering times are 6 h, 12 h, 24 h, 48 h, 96 h, and 192 h, respectively. As shown in Figure 13, it can be seen that the drawdown difference decreases with the increase of the dewatering time. When the time increases from 6 h to 48 h, the drawdown difference decreases rapidly. When the time exceeds 48 h or more, the drawdown difference decreases slowly, and finally maintains a steady balance. When the time decreases from 6 h to 192 h, the decrements of Δ/H_0 are 0.122 (S_H/H_0), 0.078 (L/H_0) and 0.072 (R_w/H_0), respectively, and the groundwater drawdown inside the pit is most significantly affected by the dewatering time. The length of the waterproof curtain and the radius of the foundation pit are weakly affected by the dewatering time.

For foundation pit dewatering with a suspended waterproof curtain, the decrement of Δ/H_0 is larger when the dewatering time is within 48 h; the data of observation wells inside and outside the foundation pit should be recorded in a timely manner to eliminate adverse effects on the foundation pit and surrounding environment. The groundwater drawdown difference of different dewatering times can be calculated by the analytical method proposed from this paper, which provides a reference for foundation pit dewatering in phreatic aquifers with a suspended waterproof curtain.

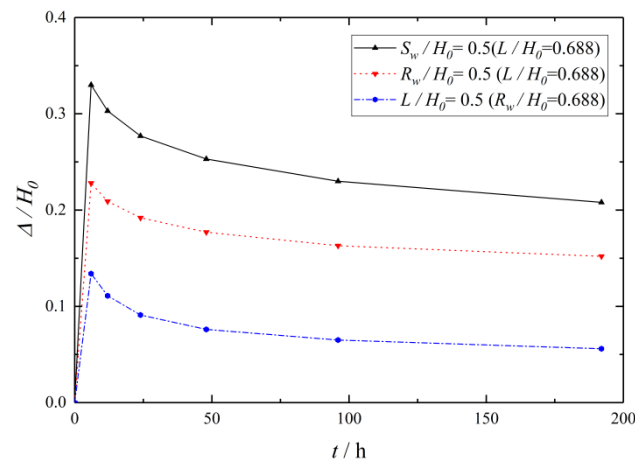


Figure 13. Effect of t on the groundwater drawdown difference.

6. Conclusions

This study obtained an analytical solution to unsteady flow with a suspended waterproof curtain and calculated the drawdown difference at various conditions. By investigating the effects of key parameters, including the groundwater drawdown inside the pit, the radius of the foundation pit, and the length of the waterproof curtain on the groundwater drawdown difference, the following conclusions are drawn:

(1) The validity of the analytical method to predict the groundwater drawdown was verified by pumping tests and FEM simulations, and the analytical method was also applicable to the calculation of dewatering with suspended waterproof curtain. This relationship between the groundwater drawdown inside and outside the pit was established, and a good consistency was found between the analytical method and FEM simulations with an error of 11.76%.

(2) Δ/H_0 increases with the increase of S_h/H_0 , and the increment of Δ/H_0 closes to 0.328. It is not suitable to adopt the scheme that the groundwater drawdown S_h exceeds the length of waterproof curtain L .

(3) Δ/H_0 decreases with the increase of R_w/H_0 . When $R_w/H_0 > 0.781$, the decrease speed becomes slower, and the scheme of decreasing of R_w/H_0 can be adopted to maintain the larger drawdown difference.

(4) The drawdown difference increases with the increase of the length of the waterproof curtain. When $L/H_0 > 0.813$, the difference tends to be stable, indicating the optimal length of the waterproof curtain to effectively maintain the drawdown difference.

(5) When the dewatering time is within 48 h, the groundwater drawdown difference decreases rapidly. When the time exceeds 48 h or more, the groundwater drawdown difference stabilizes. The field measured data of foundation pit dewatering should be recorded in a timely manner to eliminate adverse effects; the above conclusions provide references for similar cases.

Author Contributions: Conceptualization, K.Y. and C.X.; methodology, K.Y. and C.X.; software, K.Y. and M.C.; validation, K.Y., M.C. and P.W.; formal analysis, K.Y.; investigation, K.Y. and M.C.; resources, C.X.; data curation, M.C. and P.W.; writing—original draft preparation, K.Y.; writing—review and editing, C.X., M.C. and P.W.; visualization, P.W.; supervision, C.X.; project administration, K.Y.; funding acquisition, C.X. All authors have read and agreed to the published version of the manuscript.

Funding: This research was funded by [the National Science Fund for Distinguished Young Scholars] grant number [No. 51725802], [the National Natural Science Foundation of China] grant number [No. 51878276], [Joint Fund of the National Natural Science Foundation of Zhejiang Province and Huadong Engineering Corporation Limited] grant number [No. LHZ19E080001] and [Study on Long-term Performance Evolution and Big Data Analysis for Roadbed of High-speed Railways] grant number [No. U1934208].

Institutional Review Board Statement: Not applicable.

Informed Consent Statement: Not applicable.

Data Availability Statement: Not applicable.

Conflicts of Interest: The authors declare no conflict of interest.

References

1. Ng, C.; Hong, Y.; Liu, G.; Liu, T. Ground deformations and soil–structure interaction of a multi-propped excavation in Shanghai soft clays. *Geotechnique* **2012**, *62*, 907–921. [[CrossRef](#)]
2. Li, M.G.; Zhang, Z.J.; Chen, J.; Wang, J.H.; Xu, A.J. Zoned and staged construction of an underground complex in Shanghai soft clay. *Tunn. Undergr. Space Technol.* **2017**, *67*, 187–200. [[CrossRef](#)]
3. Wu, H.-N.; Shen, S.-L.; Yang, J. Identification of Tunnel Settlement Caused by Land Subsidence in Soft Deposit of Shanghai. *J. Perform. Constr. Facil.* **2017**, *31*, 4017092. [[CrossRef](#)]
4. Wang, W.; He, X. Study on the Key Technology of Marshland Foundation Pit Construction. *Geotech. Geol. Eng.* **2019**, *38*, 31–45. [[CrossRef](#)]
5. Li, M.-G.; Demeijer, O.; Chen, J.-J. Effectiveness of servo struts in controlling excavation-induced wall deflection and ground settlement. *Acta Geotech.* **2020**, *15*, 2575–2590. [[CrossRef](#)]
6. Jiao, J.J.; Wang, X.S.; Nandy, S. Preliminary assessment of the impacts of deep foundations and land reclamation on groundwater flow in a coastal area in Hong Kong, China. *Hydrogeol. J.* **2004**, *14*, 100–114. [[CrossRef](#)]
7. Zhou, N.; Vermeer, P.A.; Lou, R.; Tang, Y.; Jiang, S. Numerical simulation of deep foundation pit dewatering and optimization of controlling land subsidence. *Eng. Geol.* **2010**, *114*, 251–260. [[CrossRef](#)]
8. Tan, Y.; Lu, Y.; Wang, D. Deep Excavation of the Gate of the Orient in Suzhou Stiff Clay: Composite Earth-Retaining Systems and Dewatering Plans. *J. Geotech. Geoenviron. Eng.* **2018**, *144*, 5017009. [[CrossRef](#)]
9. Li, M.G.; Chen, J.J.; Xia, X.H.; Zhang, Y.Q.; Wang, D.F. Statistical and hydro-mechanical coupling analyses on groundwater drawdown and soil deformation caused by dewatering in a multi-aquifer-aquitard system. *J. Hydrol.* **2020**, *589*, 125365. [[CrossRef](#)]
10. Xu, C.; Yang, K.; Fan, X.; Ge, J.; Jin, L. Numerical Investigation on Instability of Buildings Caused by Adjacent Deep Excavation. *J. Perform. Constr. Facil.* **2021**, *35*, 4021040. [[CrossRef](#)]
11. Tan, Y.; Lu, Y. Responses of shallowly buried pipelines to adjacent deep excavations in Shanghai soft ground. *J. Pipeline Syst. Eng. Pract.* **2018**, *9*, 5018002. [[CrossRef](#)]
12. Lu, C.; Huang, L. Study on the Effect of Foundation Pit Excavation on the Deformation of Adjacent Shield Tunnel. *Adv. Civ. Eng.* **2022**, *2022*, 8441758. [[CrossRef](#)]
13. Sun, W.; Zhou, W.; Jiao, J. Hydrogeological Classification and Water Inrush Accidents in China’s Coal Mines. *Mine Water Environ.* **2015**, *35*, 214–220. [[CrossRef](#)]
14. Tan, Y.; Lu, Y. Forensic Diagnosis of a Leaking Accident during Excavation. *J. Perform. Constr. Facil.* **2017**, *31*, 4017061. [[CrossRef](#)]
15. Su, M.; Liu, Y.; Xue, Y.; Nie, L.; Wang, P.; Li, C.; Ma, X. Integrated geophysical detection of water inrush from foundation pit near the river: A case study of Nanjing subway station. *Environ. Earth Sci.* **2021**, *80*, 699. [[CrossRef](#)]
16. Xu, X.B.; Hu, Q.; Huang, T.M.; Chen, Y.; Shen, W.M.; Hu, M.Y. Seepage failure of a foundation pit with confined aquifer layers and its reconstruction. *Eng. Fail. Anal.* **2022**, *138*, 106366. [[CrossRef](#)]
17. Zeng, C.F.; Zheng, G.; Xue, X.L.; Mei, G.-X. Combined recharge: A method to prevent ground settlement induced by redevelopment of recharge wells. *J. Hydrol.* **2018**, *568*, 1–11. [[CrossRef](#)]
18. Liu, N.W.; Peng, C.X.; Li, M.G.; Chen, J.J. Hydro-mechanical behavior of a deep excavation with dewatering and recharge in soft deposits. *Eng. Geol.* **2022**, *307*, 106780. [[CrossRef](#)]
19. Zhang, X.Q.; Li, M.G.; Chen, J.J. Hydro-mechanical analysis of a braced foundation pit affected by rainfall and excavation in unsaturated soils. *Acta Geotech.* **2022**, 1–16. [[CrossRef](#)]
20. Peng, C.; Liu, N.; Li, M.; Zhen, L.; Chen, J. Hydro-mechanical coupled analyses on wall deformations caused by deep excavations and dewatering in a confined aquifer. *Acta Geotechnica* **2022**, *17*, 2465–2479. [[CrossRef](#)]
21. Wu, Y.X.; Shen, S.L.; Yuan, D.J. Characteristics of dewatering induced drawdown curve under blocking effect of retaining wall in aquifer. *J. Hydrol.* **2016**, *539*, 554–566. [[CrossRef](#)]
22. Wang, X.W.; Yang, T.L.; Xu, Y.S.; Shen, S.L. Evaluation of optimized depth of waterproof curtain to mitigate negative impacts during dewatering. *J. Hydrol.* **2019**, *577*, 123969. [[CrossRef](#)]
23. Zhang, X.S.; Wang, J.X.; Wong, H.; Leo, C.J.; Liu, Q.; Tang, Y.Q.; Yan, X.L.; Sun, W.H.; Huang, Z.Q.; Hao, X.H. Land subsidence caused by internal soil erosion owing to pumping confined aquifer groundwater during the deep foundation construction in Shanghai. *Nat. Hazards* **2013**, *69*, 473–489. [[CrossRef](#)]
24. Wu, Y.X.; Shen, S.L.; Wu, H.N.; Xu, Y.S.; Yin, Z.; Sun, W.J. Environmental protection using dewatering technology in a deep confined aquifer beneath a shallow aquifer. *Eng. Geol.* **2015**, *196*, 59–70. [[CrossRef](#)]
25. Tarshish, M. Modifications of Combined Mathematical Model of Flow in an Aquifer-Vertical Well System. *Ground Water* **1998**, *36*, 7–8. [[CrossRef](#)]

26. Hu, L.; Chen, C. Analytical methods for transient flow to a well in a confined-unconfined aquifer. *Ground Water* **2008**, *46*, 642–646. [[CrossRef](#)]
27. Anwar, S. A generalized model for pumping well hydraulics in confined aquifers. *J. Hydroinformatics* **2018**, *20*, 1085–1099. [[CrossRef](#)]
28. Luther, K.; Haitjema, H. An analytic element solution to unconfined flow near partially penetrating wells. *J. Hydrol.* **1999**, *226*, 197–203. [[CrossRef](#)]
29. Li, J.; Xia, X.H.; Li, M.G.; Chen, J.J.; Zhan, H. Nonlinear drainage model of viscoelastic aquitards considering non-Darcian flow. *J. Hydrol.* **2020**, *587*, 124988. [[CrossRef](#)]
30. Jacob, C.E.; Lohman, S.W. Nonsteady flow to a well of constant drawdown in an extensive aquifer. *Trans. Am. Geophys. Union* **1952**, *33*, 559. [[CrossRef](#)]
31. Pasandi, M.; Samani, N.; Barry, D. Effect of wellbore storage and finite thickness skin on flow to a partially penetrating well in a phreatic aquifer. *Adv. Water Resour.* **2008**, *31*, 383–398. [[CrossRef](#)]
32. Xu, Y.; Shen, S.; Ren, D.; Wu, H. Analysis of factors in land subsidence in shanghai: A view based on a strategic environmental assessment. *Sustainability* **2016**, *8*, 573. [[CrossRef](#)]
33. Shi, J.; Wu, B.; Liu, Y.; Xu, S.; Hou, J.; Wang, Y.; Sun, Q.; Meng, G.; Nong, Z.; Qiu, H.; et al. Analysis of the influence of groundwater seepage on the deformation of deep foundation pit with suspended impervious curtain. *Adv. Mech. Eng.* **2022**, *14*, 16878132221085128. [[CrossRef](#)]
34. Zheng, G.; Dai, X.; Diao, Y.; Zeng, C.-F. Experimental and simplified model study of the development of ground settlement under hazards induced by loss of groundwater and sand. *Nat. Hazards* **2016**, *82*, 1869–1893. [[CrossRef](#)]
35. Xu, Y.; Yan, X.; Shen, S.; Zhou, A. Experimental investigation on the blocking of groundwater seepage from a waterproof curtain during pumped dewatering in an excavation. *Hydrogeol. J.* **2019**, *27*, 2659–2672. [[CrossRef](#)]
36. Wang, J.; Liu, X.; Liu, S.; Zhu, Y.; Pan, W.; Zhou, J. Physical model test of transparent soil on coupling effect of cut-off wall and pumping wells during foundation pit dewatering. *Acta Geotech.* **2019**, *14*, 141–162. [[CrossRef](#)]
37. Luo, Z.; Zhang, Y.; Wu, Y. Finite element numerical simulation of three-dimensional seepage control for deep foundation pit dewatering. *J. Hydrodyn.* **2008**, *20*, 596–602. [[CrossRef](#)]
38. Yuan, C.; Hu, Z.; Zhu, Z.; Yuan, Z.; Fan, Y.; Guan, H.; Li, L. Numerical Simulation of Seepage and Deformation in Excavation of a Deep Foundation Pit under Water-Rich Fractured Intrusive Rock. *Geofluids* **2021**, *2021*, 6628882. [[CrossRef](#)]
39. Li, X.; Zhou, T.; Wang, Y.; Han, J.; Wang, Y.; Tong, F.; Li, D.; Wen, J. Response Analysis of Deep Foundation Excavation and Dewatering on Surface Settlements. *Adv. Civ. Eng.* **2020**, *2020*, 8855839. [[CrossRef](#)]
40. Xie, Z.; Shen, S.; Arulrajah, A.; Horpibulsuk, S. Environmentally sustainable groundwater control during dewatering with barriers: A case study in shanghai. *Undergr. Space* **2021**, *6*, 12–23. [[CrossRef](#)]
41. Zhang, X.; Wang, X.; Xu, Y. Influence of Filter Tube of Pumping Well on Groundwater Drawdown during Deep Foundation Pit Dewatering. *Water* **2021**, *13*, 3297. [[CrossRef](#)]
42. Zeng, C.; Wang, S.; Xue, X.; Zheng, G.; Mei, G. Evolution of deep ground settlement subject to groundwater drawdown during dewatering in a multi-layered aquifer-aquitard system: Insights from numerical modelling. *J. Hydrol.* **2021**, *603*, 127078. [[CrossRef](#)]
43. Vilarrasa, V.; Carrera, J.; Jurado, A.; Pujades, E.; Vázquez-Suné, E. A methodology for characterizing the hydraulic effectiveness of an annular low-permeability barrier. *Eng. Geol.* **2011**, *120*, 68–80. [[CrossRef](#)]
44. Xu, Y.; Shen, S.; Ma, L.; Sun, W.; Yin, Z. Evaluation of the blocking effect of retaining walls on groundwater seepage in aquifers with different insertion depths. *Eng. Geol.* **2014**, *183*, 254–264. [[CrossRef](#)]
45. Halek, V.; Svec, J. *Groundwater Hydraulics*; Elsevier Scientific Pub. Co.: Amsterdam, The Netherlands, 1979.
46. Sato, K.; Iwasa, Y. *Groundwater Hydraulics*; Springer: Tokyo, Japan, 2000.
47. Nishitani, T. Similarity transformation of the Boltzmann equation. *Phys. Fluids A Fluid Dyn.* **1991**, *3*, 349–355. [[CrossRef](#)]
48. Chopard, B.; Pham, V.; Lefèvre, L. Asymmetric lattice Boltzmann model for shallow water flows. *Comput. Fluids* **2013**, *88*, 225–231. [[CrossRef](#)]
49. DL/T 5213-2005; Code of Pumping Test in Borehole for Hydropower and Water Conservancy Engineering. Chinese Standard: Beijing, China, 2005. (In Chinese)